

# Accelerating Quantum Eigensolver Algorithms With Machine Learning

Avner Bensoussan<sup>1</sup>, Elena Chachkarova<sup>2</sup>, Karine Even-Mendoza<sup>1</sup>,  
Sophie Fortz<sup>1</sup>, and Connor Lenihan<sup>2</sup>

<sup>1</sup>Informatics, NMES, King’s College London, England, UK

<sup>2</sup>Physics, NMES, King’s College London, England, UK

## Abstract

In this paper, we explore accelerating Hamiltonian ground state energy calculation on NISQ devices. We suggest using search-based methods together with machine learning to accelerate quantum algorithms, exemplified in the Quantum Eigensolver use case. We trained two small models on classically mined data from systems with up to 16 qubits, using XGBoost’s Python regressor. We evaluated our preliminary approach on 20-, 24- and 28-qubit systems by optimising the Eigensolver’s hyperparameters. These models predict hyperparameter values, leading to a 0.13%-0.15% reduction in error when tested on 28-qubit systems. However, due to inconclusive results with 20- and 24-qubit systems, we suggest further examination of the training data based on Hamiltonian characteristics. In future work, we plan to train machine learning models to optimise other aspects or subroutines of quantum algorithm execution beyond its hyperparameters.

## 1 Introduction

Modern-day *Noisy Intermediate-Scale Quantum* (NISQ) devices are the current state-of-the-art in *Quantum Computing* (QC) characterised as noisy with an intermediate scale in terms of the number of qubits they have [43, 10, 1]. These devices have not yet evolved to support fault-tolerant calculations with a large enough number of qubits to achieve quantum advantage. However, these already enable quantum researchers and engineers to develop, optimise and test various quantum algorithms. In this interim time of intensive hardware development, robust and innovative quantum algorithms [34] provide a way to tackle the limitations of the current quantum processors. One of the most promising applications of QC is in the field of quantum chemistry for molecular simulations, structure design, drug design and more [37, 33, 35]. A prominent example of a class of quantum algorithms that is rapidly evolving in the field of quantum chemistry is the *Variational Quantum Eigensolver* (VQE) [51], which aims at estimating the ground state energy of Hamiltonians. Different types of VQE algorithms are being developed and tailored for various systems.

Whilst taking part in the Quantum Algorithm Grand Challenge [46] organised by QunaSys<sup>1</sup> [44], we tackle an instance of quantum algorithms for eigensolving, designed to estimate the eigenvalues and eigenvectors of a given Hamiltonian to find its ground state energy. Our approach focuses on applying machine learning algorithms to explore and optimise quantum algorithms to achieve potential advancements in quantum eigensolving and improve the performance and accuracy of quantum algorithms for larger system setups that are currently too complex to tackle. Our first attempt at the problem was to find a methodology to select the best hyperparameters for the ADAPT-QSCI quantum algorithm [32] that minimise the runtime and the final result for the ground state energy through using machine learning techniques trained on smaller systems [13]. This method is not specifically tailored to ADAPT-QSCI and can be applied to any *Quantum Eigensolver*-based algorithm. Next, we applied the *Quantum Complex Exponential Least Squares* (QCELS) algorithm [17] to the problem. We investigated the suitability and limitations of the QCELS algorithm when applied to large systems [14].

---

<sup>1</sup>QunaSys is a technology company aiming to achieve QC’s full potential through algorithm development into product engineering

In the evaluation, we have assessed their performance and potential benefits for solving 16 quantum systems of 20-, 24- and 28-qubits, showing limited minor improvement for 20- and 28-qubit systems.

The rest of the paper is structured as follows. [Section 2](#) lists related work in the field and [Section 3](#) focuses on the background of the quantum computing algorithms that we have investigated, software engineering optimisation methods and machine learning, followed by a deeper dive into the methodologies of quantum eigensolver algorithms in [Section 4](#), and machine learning applications to accelerate quantum algorithms in [Section 5](#). In [Section 6](#), we present the experiment’s methodology and our results. Our conclusions can be found in [Section 7](#), including notes containing references to the source code used in the paper and the relevant data and acknowledgements.

**A note on the 2024 Quantum Algorithm Grand Challenge (QAGC2024).** The challenge focused on improving current quantum algorithms for the problem of finding the ground state energy of a one-dimensional orbital rotated Fermi-Hubbard model Hamiltonian using a given 28-qubit system in the most optimal way [46]. The aim of the challenge is to design an algorithm, given specific constraints (*i.e.* the number of shots of  $10^7$ , timeout of  $6 \times 10^5$  seconds and limited input data), that can output the closest answer to the actual ground state energy. Previous year’s challenge [45] had the same aim but was based on a much smaller 8-qubit system. The winning algorithm was the company’s proposition later published as Quantum-Selected Configuration Interaction (QSCI) [32].

## 2 Related Work

**Quantum Computing.** Quantum Computing (QC) was conceptualised initially to simulate quantum mechanics using computers “*built of quantum mechanical elements which obey [the] quantum mechanical law*” [22]. Later, it was found that QC could have several potential applications and offer significant speed-up over classical computing [5, 4, 16, 6, 27, 11]. In 1994, Shor’s proposal of a polynomial-time algorithm for prime factorization and discrete logarithms on a quantum computer raised enormous interest due to its potential threat to modern RSA cryptosystems [49]. Soon after, Grover introduced a fast database search on quantum computers that promised quadratic speed-up over the best classical algorithm [27]. The resulting potential speed-up is often referred to as “quantum supremacy” [3]. Several studies have applied software engineering techniques to optimise quantum computing [24, 25], while testing and debugging approaches have been found to be beneficial in quantum software development [39, 59].

**NISQ.** Demonstrating quantum supremacy on real hardware remains a long-standing challenge, especially at a scale where quantum devices would solve real-life calculations. Although quantum supremacy seems difficult to achieve soon, NISQ algorithms are a prominent example that hybrid systems combining small quantum circuits with classical computations could present some computational advantages, *i.e.*, a quantum advantage [43]. Most agree this stage of QC will likely last for the next few years if not decades, and refer to it as the NISQ era [43]. Variational Quantum Algorithms (VQA) are the most common example of an efficient combination of a reduced quantum circuit inside a classical optimisation loop [51].

**Machine Learning.** Machine Learning (ML) algorithms are increasingly used to improve and automate software engineering tasks [55, 58, 28, 48, 19], especially after the advent of Large Language Models (LLM), with common applications in software engineering, including optimisation, code generation, bug detection and automated testing [20, 53, 12, 9, 15, 30]. Furthermore, connections between Machine Learning and QC have been broadly explored, both to optimise Machine Learning with QC and to optimise QC with Machine Learning [21, 41, 54]. As we aim to optimise the quantum algorithm hyper-parameters classically, we discuss how we apply machine learning to enhance the software engineering aspects of our approach in [Section 5](#).

## 3 Background

Our approach combines machine learning, search-based software engineering, and quantum physics to accelerate quantum algorithms, specifically eigensolvers. We provide background on each area before

discussing the applications of machine learning in quantum algorithms. In [Section 4](#), we discuss the implementation of the eigensolvers used in this research.

### 3.1 Variational Quantum Algorithms

Variational Quantum Algorithms (VQA) are among the most promising examples of NISQ algorithms [\[51\]](#). The main goal of a VQA is to find the optimal parameters for a parameterized quantum circuit, leading to a solution for a given computational problem. We provide an overview of the structure and functioning of a VQA.

1. *Problem definition.* The first step involves defining a computational problem that can benefit from quantum processing and translating it into an objective or cost function. In most applications, it consists of a Hamiltonian construction and representation of a quantum system.
2. *Optimisation process.* A parameterized quantum circuit, known as the variational ansatz, is designed. This circuit contains gates with adjustable parameters, denoted as  $\theta$ . A quantum state  $|\psi(\theta)\rangle$  is measured, and the outcomes are used to compute the expectation value of the cost function  $\langle\psi(\theta)|H|\psi(\theta)\rangle$ .  $H$  is the Hamiltonian of the quantum system, and the expectation value of this Hamiltonian is the cost function.
3. *Convergence check and output* The optimisation process continues until a convergence criterion is met, indicating that further iterations are unlikely to significantly improve the solution. This convergence check ensures that the algorithm has reached a stable and potentially optimal solution. The final set of optimised parameters  $\theta_{opt}$  represents the solution to the quantum problem. This solution can be used for further analysis or as the output of the VQA.

An in-depth explanation and a detailed figure can be found in the work of Bharti et al. [\[10\]](#).

**VQE and ADAPT-VQE.** Variational Quantum Eigensolvers (VQE) were introduced in 2014 by Peruzzo et al. [\[42\]](#). It is the most popular VQA, and aims to approximate the ground state energy of a quantum system iteratively. Although considered among the most promising NISQ algorithms, VQEs present several limitations. VQE optimisations have been widely investigated, from classical optimisers, to measurement strategies and Ansatz structure [\[51\]](#). One popular algorithm derived from VQEs is the ADAPT-VQE [\[26\]](#). The main distinction is the restructuring of the Ansatz at each iteration. A pool of operators is defined from which operators are selected to update the ansatz during the optimisation process. ADAPT-VQEs are found to have more precise results in some applications, at a cost of a higher computational load.

### 3.2 Use of AI with GI and Search-based Optimisation

In this work, we integrate ML with search-based methods. We first use predictions on smaller systems, utilising the cost function values of a Hamiltonian of smaller systems and randomly generated hyperparameters of the quantum algorithm to train a gradient boosting model to predict the cost function value. We then use this model to explore and optimise hyperparameters for a larger Hamiltonian system, which is costly to solve classically, via a crossover operator.

**Search-based Optimisation and Genetic Improvement (GI).** Search-based methods [\[29\]](#) have also been used for optimisation tasks to find the best possible subset of requirements. The optimisation, in the case of the quantum algorithm’s hyperparameters, aims to save precious resources like the number of shots but mainly to achieve a closer prediction to the system’s ground state energy<sup>2</sup>, influenced by the selection of optimal hyperparameters (i.e. a minimum of the cost function approximating the lowest energy level, [Subsection 3.1](#)).

These methods aim to find the near-optimal solution iteratively, ending when a stopping condition is met (e.g. reaching a maximum number of iterations). Starting with a set of candidate solutions, they are evaluated using a fitness function. GI then diversifies solutions over iterations through mutation

---

<sup>2</sup>The lowest energy level, which for eigensolvers is the lowest eigenvalue that is the value associated with the lowest eigenvector of the problem, see [Section 4](#).

operations like bit flip (on a single solution) or crossover (on multiple solutions) to potentially generate better-performing offspring. The method can occasionally minimise the population or inject noise to avoid converging to local minima (or maxima, depending on the problem). Using ML to estimate the fitness function is common when direct evaluation or computation is infeasible. We utilise this idea for larger Hamiltonians in [Section 5](#).

In the context of this work, we define a solution as an assignment of hyperparameters (their values based on some pre-defined constraints, e.g. `sampling_shots` are between 100 to  $10^6$ ), with the best solution being a global minimum. Consequently, our fitness function is related to the lowest energy level for a specific assignment of the hyperparameters and Hamiltonian. We perform these stages classically as quantum computations are costly. However, the final estimation of the quantum algorithm’s cost function is done using a quantum simulator with the optimised hyperparameters.

**Machine Learning.** ML, a branch of artificial intelligence (AI), aims to learn from data and generalise models via statistical algorithms (e.g. random forest or linear regression) to identify patterns and make predictions and decisions on new, unseen data. The process typically involves several main phases: data collection, data pre-processing (including data augmentation and mining), model training, and model prediction (or deployment).

In this work: Data consists of Hamiltonians, parameters and the lowest energy levels. We collect data from smaller quantum systems (e.g. 2-qubit, 4-qubit) to build a model for larger systems (20-qubit and above). Data is gathered from online sources or computed via simulations or classical algorithms. The data is then processed and augmented to ensure compatibility with machine learning models, aiming to keep relevant features of the physical system for training. We discuss our choices with respect to data collection, augmentation, and model prediction in [Section 5](#).

**Gradient Boosting.** The Gradient Boosting technique [\[23\]](#) is a supervised learning method suitable for regression and classification. It efficiently handles large amounts of data, real numbers, and datasets with many features, as is the case here when representing the Hamiltonian in our dataset, which even with aggressive approximation may result in large data instances. The resultant prediction model allows prediction with large datasets with high precision, avoiding flat predictions caused by scaling issues or oversimplified predictions due to insufficient data relative to the number of features.

**XGBoost Library.** We employ XGBoost (eXtreme Gradient Boosting), an open-source Python library of the Gradient Boosting framework [\[57\]](#), as a regressor to predict a response variable, in our case, the lowest energy level of the quantum system (the Hamiltonian). The input features for our model include the Hamiltonian, the number of qubits, and a set of hyperparameters.

## 4 Quantum Eigensolver Algorithms

During our experiments and development of the solution to the challenge, we used and wrote two implementations of *Quantum Eigensolver* (QE), ADAPT-QSCI and QCELS, described in [Subsection 4.1](#) and [Subsection 4.2](#). QEs aim to find the nearest approximation of the eigenvalues and eigenvectors of a given system (i.e. the input Hamiltonian). Furthermore, in QC, we aim to determine the ground state energy of the system (the lowest energy level), similarly to the challenge [\[46\]](#).

In our evaluation, we used the implementation of ADAPT-QSCI provided by the challenge scripts [\[46\]](#) and implemented our own QCELS solver. Each implementation can run on a classical simulator (i.e. classic mode) or a NISQ (i.e. QC mode). In classical mode, we are limited by the size of the system and probably can run up to 20-qubit systems at most. In our experiments, we limited our classical mode runs to 16-qubit systems.

Next, we describe the two QE algorithms used in this work.

### 4.1 ADAPT-QSCI Algorithm

**QSCI.** Quantum-selected configuration interaction (QSCI) method is a computational algorithm in quantum chemistry that is used for calculating electronic structure of molecules in an intelligently chosen subspace that makes larger systems feasible to study on modern-day NISQ devices [\[31\]](#). A full configuration interaction (FCI) requires high computational cost and memory usage that is out of

reach for large systems but by using QSCI the computational space can be reduced through selecting only the most important configurations (ways of distributing electrons among molecular orbitals) by a pre-selection algorithm. One such algorithm is ADAPT-QSCI [40].

**ADAPT-QSCI.** Adaptive Construction of Input State for Quantum-Selected Configuration Interaction (ADAPT-QSCI) is an iterative algorithm that uses a predetermined pool of single Pauli operators  $\mathbb{P} = \{P_1, \dots, P_T\}$  that are generators of rotation gates for the input quantum state of QSCI, and selects the best operators from the pool to lower the energy output by QSCI. The operator pools are similar to ADAPT-VQE approaches and could be based on fermionic or qubit excitations. In this method a simple sampling measurement is performed on an input state prepared by a quantum computer - this is the only step that requires quantum computation. The measurement result is used for identifying the most important electron configurations for performing the selected configuration interaction (CI) calculation on classical computers, that is, Hamiltonian diagonalization in the selected  $R_k$  dimensional subspace  $S_k = \text{span}\{|r_1^{(k)}\rangle, \dots, |r_{R_k}^{(k)}\rangle\}$  [40]. QSCI relies on a quantum computer only for generating the electron configurations via sampling, and the subsequent calculations to output the ground-state energy and the pool operator gradients  $h_j = \langle c_k | i[H, P_j] | c_k \rangle$  are executed on classical computers<sup>3</sup>. These calculations are made possible on classical machines due to the reduction of the dimensionality of the subspace based on QSCI. The quantum advantage of the ADAPT-QSCI stems from the potential speed up and improved precision of the generating of the electron configurations via sampling.

## 4.2 Quantum Complex Exponential Least Squares (QCELS) Algorithm

To go beyond NISQ algorithms, where typically the QC is used to simply prepare an ansatz state and then measured in a Pauli basis, we used the Quantum Complex Exponential Least Squares algorithm (QCELS) [17] which uses a controlled time evolution unitary and so introduces a large number of two-qubit gates. However, it does not suffer from the barren plateau problem of VQE and is low enough depth that it will likely be run on early QCs with some error correction, offering a good solution when the number of qubits is too large for NISQ algorithms.

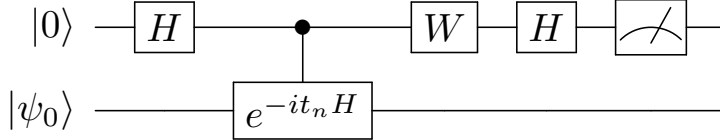


Figure 1: QCELS circuit [17]

The QCELS algorithm [17] takes a reference state  $|\psi_0\rangle$  and evolves it by the time evolution operator  $U(t) = e^{-iHt}$  enclosed within a Hadamard test (as depicted by Figure 1). If the reference state is the ground state ( $|\phi_0\rangle$ ) then the resultant expectation values will have a single frequency  $Z_n = \langle \phi_0 | U(t_n) | \phi_0 \rangle = e^{-iE_0 t_n}$ , where  $E_0$  is the ground state energy. If the reference state,  $|\psi_0\rangle$ , is not exactly the ground state then the resultant function is  $Z_n \approx \langle \psi_0 | U(t_n) | \psi_0 \rangle = \sum_i p_i e^{-iE_i t_n}$  where  $p_i = |\langle \phi_i | \psi_0 \rangle|^2$  is the probability of measuring the eigenstate  $|\phi_i\rangle$  of the Hamiltonian. Thus, if a reference state with good overlap with the true ground state is known, we can apply the time evolution operator within a Hadamard test  $N$  times and fit to the resulting complex exponential. For this challenge, we found that the provided Hamiltonians had an initial Hartree-Fock ground state that retains an overlap with the true ground state - up to 28 qubits - to extract a good estimate of the energy. The time evolution operator was implemented with a first-order Trotter-Suzuki expansion with Hamiltonian truncated to only the Pauli operators with the largest 200 coefficients to reduce gate count.

Our procedure for fitting a sum of exponentials to the collected data was to initially fit with a single frequency fitting to

$$f_{\text{fit}}^{(1)} = r_1^{(1)} e^{-i\theta_1^{(1)} t} + 1 - r_1^{(1)}, \quad (1)$$

<sup>3</sup> $|c_k\rangle$  is a state corresponding to classical vector  $c_k = \sum_{l=1}^{R_k} (c_k)_l |r_l^{(k)}\rangle$ , and  $i[H, P_j]$  is calculated through projecting onto the subspace  $S_k$  and evaluating the expectation classically using the classical vector  $c_k$ . [40].

before using this frequency as an initial guess and then adding sequentially second and third frequencies,

$$f_{\text{fit}}^{(2)} = r_1^{(2)} e^{-i\theta_1^{(2)} t} + r_2^{(2)} e^{-i\theta_2^{(2)} t} + 1 - r_1^{(2)} - r_2^{(2)} \quad (2)$$

$$f_{\text{fit}}^{(3)} = r_1^{(3)} e^{-i\theta_1^{(3)} t} + r_2^{(3)} e^{-i\theta_2^{(3)} t} + (1 - r_1^{(3)} - r_2^{(3)}) e^{-i\theta_3^{(3)} t} \quad (3)$$

which were constrained to be smaller in magnitude than the initial fitted frequency  $\theta_1^{(1)}$  to ensure that they acted as corrections to the initial fit, for the purpose of the challenge we also added a factor 0.8 to keep the fitting procedure as safe as possible due to the need for it to be automated. The size of the amplitude  $r_2^{(2,3)}$  is also constrained to be smaller than  $r_1^{(1)}$ .

The outcome of this procedure when applied to test data collected from an example of the orbital rotated Hubbard Hamiltonian on 28 qubits is given in figure [Figure 2](#), with a sequential improvement towards the correct answer as we increase the number of frequencies in the fit.

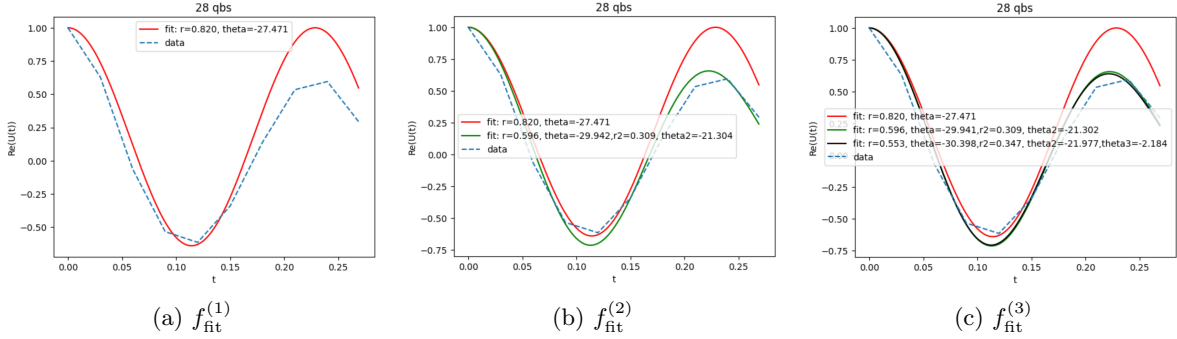


Figure 2: QCELS results from sample data of the orbital rotated Hubbard Hamiltonian on 28 qubits (various parameters)

## 5 Accelerating Quantum Algorithms with Machine Learning

In the previous section, we explored two implementations of the QE algorithms: ADAPT-QSCI and QCELS. Building on these foundations, we now introduce our proposed solution, the prototype of which was submitted to the QAGC challenge [46]. Our approach enhances ADAPT-QSCI and QCELS by integrating machine learning techniques to optimise their hyperparameters. Before presenting our solution, we explain how we gather sufficient data to train an ML model ([Subsection 5.1](#)). We then present our solution in detail ([Subsection 5.2](#)), followed by implementation details and the constraints set by the QAGC challenge rules ([Subsection 5.3](#)). In the evaluation, we demonstrate that quantum algorithms can benefit from incorporating a machine learning model to improve decision-making and overall performance ([Section 6](#)).

### 5.1 Data Augmentation

ML algorithms operate in two primary phases: training and prediction. During the training phase, a sufficiently large dataset is essential for making probabilistic generalisations. In a supervised learning context, this dataset comprises instances where the true output values are known. Once the model is trained, it can make predictions on new, unseen data. The quality and accuracy of the training dataset directly influence the effectiveness of these predictions. Consequently, our initial challenge was to obtain a robust initial dataset.

Acquiring a sufficiently large dataset is a significant challenge. One common solution to this problem is *data augmentation*, a technique that involves creating additional training data from the existing dataset through various transformations. These transformations can include rotations, scaling, cropping, and other modifications that simulate new data samples, thereby enhancing the diversity and volume of the training dataset. The effectiveness of data augmentation has been extensively studied and validated in numerous literature reviews (*e.g.*, [36, 38, 52, 50, 56]).

The accuracy and generalisation of an ML model are closely linked to the size of the dataset. In the context of quantum simulation data, each data instance encompasses numerous features due to



Figure 3: Classical pre-processing phase - training a regressor on smaller systems

the substantial memory required to represent the Hamiltonian. To generate a sufficiently large dataset for training, we utilise a classical state vector simulator rather than a quantum device, as quantum computing time is prohibitively expensive. This simulator allows us to compute the exact energy levels of smaller Hamiltonians (*i.e.* fewer than 28 qubits) with high precision. Each data instance in our training dataset encompasses the complete set of information required for the quantum problem, including the Hamiltonian<sup>4</sup>, its exact energy level, and the hyperparameters used to compute this level.

We use this dataset to train our ML model and predict hyperparameters for new Hamiltonians. We anticipate that the generalisation capabilities of deep learning will enable our model to handle larger Hamiltonians and predict hyperparameters for unseen 28-qubit problems effectively. This approach adheres to the challenge rules outlined in [Subsection 5.3](#), as we do not apply classical methods to Hamiltonians of 28 qubits or larger. Further details on the dataset structure and mining processes are discussed in the *Data Preparation* stage described in [Subsection 5.2](#).

Note on the energy levels predictions: As energy levels are real numbers (*i.e.*, are in a continuous domain), classification might result in precision issues during the prediction phase. Moreover, the exact energy level value is irrelevant as we do not use these values directly. We are interested in knowing whether certain data (Hamiltonian and some quantum-system-related parameters) lead to further minimised answers (the lowest energy level value). This is the relationship between these values. Therefore, we have used a regressor to predict roughly the lowest energy levels.

## 5.2 AccelerQ

In this section, we present **AccelerQ**, our approach for enhancing quantum algorithm performance through hyperparameter optimisation. We employ a search-based methodology to identify the optimal combination of hyperparameters by leveraging a regressor trained on smaller systems. This regressor estimates system energy, which serves as the fitness function in our optimisation process. Below, we provide an overview of the methods employed, including search-based techniques, the regressor, and its Python implementation.

[Figure 3](#) illustrates our hyperparameter optimisation algorithm for quantum problems, which utilises a regularizing gradient boosting regressor (XGBoost). The process is organised into three key stages: data preparation, model training, and hyperparameter optimisation. This algorithm generates tailored hyperparameter suggestions for executing the QE algorithm, customised for each specific Hamiltonian.

To ensure the generalisability of **AccelerQ** and its applicability to various QE algorithms (*e.g.*, ADAPT-QSCI or QCELS), we have developed a versatile wrapper. This wrapper encompasses the Hamiltonian, the number of qubits, a parameter indicating whether the computation should be performed classically or on a quantum computer, and the hyperparameters (of both: the QE and ML problems, while we only optimise here those of the QE problem). In our evaluation (see [Section 6](#)), we applied **AccelerQ** to the ADAPT-QSCI and the QCELS algorithms.

<sup>4</sup>In practice, we do not include in our data the Hamiltonian as-is but a compressed representation of the Hamiltonian to save memory and avoid overfitting. Compressing a Hamiltonian in the context of QC reduces the complexity of the Hamiltonian operator but keeps the essential physical properties of the system. We compressed by truncating small terms.

**Data Preparation.** We add open-source commonly used molecular Hamiltonians (H<sub>2</sub>O, LiH, BeH<sub>2</sub>, Hemocyanin [2], and H chain) and combine them with the ones provided by the challenge Hamiltonians of 16 qubits or less, details in [7]. The wrapper is run in classical mode while giving a randomly generated set of hyperparameters each time, recording the energy level as the score. This process is repeated to produce a data array for training a Regularising Gradient Boosting Regression (XGBoost). The generated data—consisting of a compressed Hamiltonian and hyperparameter vectors (Xs) and their corresponding energy levels (Ys)—is stored for further processing. This stage corresponds to the first of the three steps depicted in Figure 3. We utilise a classical eigensolver during data preparation (Subsection 5.1).

**Model Training.** Our algorithm uses an XGBoost model to predict the best hyperparameters. Before training, it ensures that all data vectors are of consistent length by padding them as needed. The padded data array is split into training and testing sets. The model is then trained, tested, and evaluated for performance. The training of the XGBoost model corresponds to the fourth step of Figure 3.

**Hyperparameter Optimisation.** With the XGBoost model trained, the algorithm proceeds to predict the optimal hyperparameters for a given Hamiltonian of 28 qubits (Figure 3, fifth step). It generates a series of hyperparameter vectors and uses the XGBoost model to predict their performance. In each iteration (generation), the best-performing vectors are selected (i.e. predicted to have minimum score value). A crossover operator combines pairs of these vectors, generating new hyperparameters through averaging, extremes, and random values. In the last generation, the vector with the minimum score (predicted energy level) is returned as the optimal set of hyperparameters. Finally, the algorithm runs ADAPT-QSCI with the optimised hyperparameters (Figure 3, sixth and last step).

### 5.3 Implementation Details

Our implementation is divided into three parts (data collection, training and optimisation) and is written in Python 3.10.12. The rest of the requirements are derived from the rules of the 2024 Quantum Algorithm Grand Challenge (QAGC2024), with one exception: we utilised GPU during the training phase of our models while keeping them relatively small to be able to deploy them on desktop CPU. We used the Python library *QURI Parts*<sup>5</sup> to simulate and access QC.

**Quantum Algorithm Grand Challenge Description.** Participants in the 2024 Quantum Algorithm Grand Challenge (QAGC2024) were tasked with challenging the ADAPT-QSCI Algorithm [40], a quantum-classical hybrid approach designed to compute the ground states and energies of many-body quantum Hamiltonians (Subsection 3.1). The challenge specifically focuses on optimising a quantum algorithm for solving a 28-qubit system under several constraints (see full list [47]). These constraints included a specific machine specification (CPU, 16 GB RAM), a practical time limit of  $6 \times 10^5$  seconds to ensure all solutions could be evaluated within a reasonable timeframe and a shots limit of  $10^7$  due to the high cost of quantum computer execution. Participants were required to make essential use of quantum computers, as the goal was a quantum competition, and current classical algorithms do not scale efficiently for systems with 28 or more qubits.

Furthermore, participants were instructed to output only the energy level of the ground state, calculated using the quantum algorithm of choice. Exact calculations of the ground-state energy using methods like the Bethe ansatz were prohibited, as such methods do not scale well for larger systems (28 qubits or more). Additionally, participants were not allowed to hard-code initial parameters or hyperparameters to ensure adaptability to new Hamiltonians. That constraint ensured that the proposed solution is generic and not tailored for a specific Hamiltonian or subset of problems.

To facilitate the automatic evaluation of all participants’ solutions, the contest organisers provided a specific structure for their responses, limiting participants to modifying a single `answer` file. While this constraint streamlined the evaluation process, it also introduced certain limitations. Notably, it prevented us from leveraging the full potential of machine learning techniques, as models could not be stored globally and had to be retrained for each evaluation. Although this approach was effective for the contest evaluation, it is not ideal for software engineering practices that prioritise modularity.

---

<sup>5</sup><https://pypi.org/project/quri-parts/>



A more effective strategy would be to divide the problem into distinct stages, each with its own constraints. Constraints provided by the contest organisers are particularly relevant for the prediction phase but may not be suitable for the training phase. Recognising these limitations, in future iterations of our solution we plan to adopt further a more flexible approach, allowing for greater use of advanced methods and better adaptability, while respecting the original framework and intentions set by the challenge organisers.

## 6 Evaluation

We evaluated `AccelerQ` for its ability to further optimise ADAPT-QSCI and QCELS algorithms by suggesting better hyperparameters tailored per system.

### 6.1 Methodology

We demonstrated our idea on the optimisation of hyperparameters of two quantum eigensolver algorithms. We used 4- to 16-qubit systems to train the models. We deployed the models on 20-, 24- and 28-qubit systems. We aim to understand:

**RQ1:** To what extent can `AccelerQ`'s optimisation of hyperparameters alone accelerate and improve the efficiency and accuracy of Quantum Eigensolver (QE) algorithms on NISQ devices in terms of runtime, error, and system size?

Given that we extract a model from smaller systems up to 16 qubits, we wish to assess the scalability of these models and to test if we have reduced performance as the system gets larger, that is:

**RQ2:** How scalable are machine learning-predicted hyperparameters learned on smaller systems when applied to QE algorithms for Hamiltonian systems with increasing qubit number and complexity?

In our evaluation, we applied our methodology to 16 larger systems of 20-, 24- and 28-qubit with known lowest energy levels, using the two QE implementations: ADAPT-QSCI and QCELS (Section 4) to answer RQ1 and RQ2.

We constructed two models—one for each implementation—using data extracted classically (Section 4) from up to 16-qubit systems. The data extraction and model training were general. The resultant model aimed to predict the optimal hyperparameters for its QE implementation and a system (Hamiltonian). The optimisation process took an implementation, its trained model and a system (a problem to solve) as input and returned the optimal hyperparameters for this setup.

**Baseline and Parametrisation.** Our evaluation baseline is the results obtained with an implementation's default hyperparameters, fixed across all systems in the evaluation. The hyperparameters were specific per implementation, were optimised, and their performance was compared against the baseline. Apart from the hyperparameters, ADAPT-QSCI and QCELS implementations were provided with `ham` and `number_qubits`, the input system and the required number of qubits for the corresponding Hamiltonian, and the flag `is_classical` being set to `True` during the data collection phase, and either `True` or `False` otherwise (classical or QC). We did not optimise this part.

**ADAPT-QSCI.** The ADAPT-QSCI implementation [40] includes several hyperparameters that control its operation. These hyperparameters have default values, which we used as our baseline for comparison. `num_pickup` (default: 100) and `coeff_cutoff` (default: 0.001) parameters control the terms retained or removed from the Hamiltonian compressed representation. `self_selection` indicates whether self-selection is enabled (default: `False`), which forces the algorithm to work in subspace. `iter_max` is the maximum total number of iterations (default: 100). `sampling_shots` is the number of sampling shots for measurements per iteration (default:  $10^5$ ). `atol` is the absolute tolerance for convergence criteria (default:  $1e - 6$ ). `final_sampling_shots_coeff` is the number of shots for the calculations if the same operator appears twice or the operator parameter is close to zero (default: 5). `num_precise_gradient` is the number of operators from the pool to calculate gradient more precisely (default: 128). `max_num_converged` specifies the maximum number of iterations within `atol` needed for a solution to be considered converged (default: 2). `reset_ignored_inx_mode` specifies after how many iterations previously used operators can be reused (default: 0). These default values are the

baseline for configuring the ADAPT-QSCI implementation, but these can be overridden (e.g.) when using `AccelerQ` suggestions tailored per system.

**QCELS.** The QCELS hyperparameters are a different set of arguments. This includes the following: `ham_terms` is the number of individual terms that are retained in the Hamiltonian after truncation. The Hamiltonian is transformed to a qubit Hamiltonian formed from a linear combination of Pauli strings, the truncation then retains the largest `ham_terms` of these and the rest are discarded. The default value is set to be 200 and we search for its optimal value between `random.randint(50, 1000)`. `ham_cutoff` is the same as `coeff_cutoff` in ADAPT-QSCI implementation, setting a minimum value for the retained coefficients, discarding all terms in the Hamiltonian with coefficients lower than this threshold. `delta_t` is the time step for the simulation or evolution of the system (the default is 0.03; `delta_t = random.uniform(1e-3, 0.3)`), the expectation value of the time evolution operator is calculated at a set of times starting from zero and separated by this value. `n_Z` is the total number of points used in fitting the time evolution and so `n_Z-1` is the total number of points at which the expectation value is evaluated. The default value is 10; `n_Z = random.randint(5, 25)`. `alpha` is a scalar parameter that determines how much smaller the parameters  $r_2^{(2)}$ ,  $\theta_2^{(2)}$  and  $r_2^{(3)}$ ,  $\theta_2^{(3)}$ ,  $\theta_3^{(3)}$  are forced to be than (default is 0.8 ;`alpha = random.uniform(0.5, 1)`).

Using the above, we defined different types of hyperparameter vectors per implementation. The input vectors ('X's) were normalised to the size of vectors in 28-qubit systems and included the implementation hyperparameters and the system's Hamiltonian. The Hamiltonians were compressed by removing small elements (`abs(0.05)` and below). The target values (Y's) represent the predicted lowest energy levels. Note: since we utilised the classical mode when extracting data from smaller systems, these are rough approximations, not the true values.

## 6.2 Experimental Setup

We extracted 66 files for the training phase using classical wrappers (i.e. 33 for ADAPT-QSCI and 33 for QCELS). We used *open-source molecular Hamiltonians*—smaller systems prepared as discussed in the data preparation paragraph in [Subsection 5.2](#)— and *the challenge Hamiltonians*—the Hamiltonians of 04 and 12 qubits for seeds `_00` to `_04` from [\[44\]](#).

We trained the ADAPT-QSCI with 4760 records (small dataset) and QCELS with 14510 records (medium dataset), out of which 400 and 5550 records (respectively) with the challenge Hamiltonians. Per system sizes of 4-, 6-, 7-, 8-, 10-, 12-, 14-, and 16-qubit, we utilised 60, 750, 500, 500, 1500, 450, 800 and 200 records for ADAPT-QSCI hyperparameters, and 60, 750, 500, 500, 1000, 6600, 2100 and 3000 for QCELS hyperparameters, respectively. The QCELS implementation ran faster than ADAPT-QSCI, allowing us to extract a medium-sized dataset for QCELS. The models were trained using `XGBRegressor`<sup>6</sup>, version 2.1.1 of the `XGBoost` library, on a single GPU core, NVIDIA 12GB PCI P100 GPU, 12 GB VRAM, running Ubuntu 22.04.4 LTS. We deployed the model on an ARM M2 Mac running Ubuntu 22.04.4 with 8 GB RAM.

We evaluated on a quantum simulator the predictions for several Hamiltonians of 20-, 24-, and 28-qubit systems with a known real answer (the challenge Hamiltonians were 20 and 28 qubits for seeds `_00` to `_04` [\[44\]](#); the rest of the seeds were open-source molecular Hamiltonians [Subsection 5.2](#)). We ran the simulations on a single virtual machine with 16 virtual CPU cores and 32 GB RAM running Ubuntu 20.04.2 LTS `x86_64`. The host had a single AMD EPYC 7313P CPU (single socket, 3.0 GHz, 16 cores, 2 threads per CPU).

## 6.3 Results

The models for ADAPT-QSCI and QCELS were trained with dataset sizes of 757 MB and 4868 MB, respectively. The model sizes were 1.1 MB for ADAPT-QSCI and 2.86 MB for QCELS.

We first evaluated the model performance by calculating the mean absolute error (MAE) and the mean squared error (MSE) of two testing sets. We sampled 10% of data from each system (first testing set) and split the remaining data into training and (second) testing sets at an 80% - 20% ratio. We had no validation stage due to (1) the limited number of systems with known Y's value (typically

<sup>6</sup>[https://xgboost.readthedocs.io/en/latest/python/python\\_api.html#xgboost.XGBRegressor](https://xgboost.readthedocs.io/en/latest/python/python_api.html#xgboost.XGBRegressor)

Table 1: Predicted optimal hyperparameters (A-J col.) with the first row stating the default values for ADAPT-QSCI implementation (**Size**: the approximate size of the Hamiltonian as a vector of terms, **A**: num\_pickup, **B**: coeff\_cutoff, **C**: self\_selection, **D**: iter\_max, **E**: sampling\_shots, **F**: atol, **G**: final\_sampling\_shots\_coeff, **H**: num\_precise\_gradient, **I**: max\_num\_converged, and **J**: reset\_ignored\_inx\_mode)

System	Size	A	B	C	D	E	F	G	H	I	J
Default	-	100	0.001	0	100	100000	1.00E-06	5	128	2	0
20qubits_00	63636	985	7.64647e-03	0	344658	49458	5.67168e-05	3	77	2	1
20qubits_01	54717	807	9.41494e-03	1	382109	964853	9.00118e-05	6	79	2	64
20qubits_02	54723	934	4.56117e-03	0	478268	875460	4.27314e-05	8	294	3	83
20qubits_03	54710	551	1.13139e-03	1	802530	106374	7.23056e-05	1	161	2	79
20qubits_04	63636	182	4.06265e-03	0	398085	61950	7.69414e-05	7	194	4	11
20qubits_05	46	593	8.46933e-04	1	278431	148423	6.66628e-05	7	158	4	58
24qubits_05	56	67	7.77741e-03	1	655715	676443	3.37411e-05	8	176	2	89
24qubits_06	56	292	4.00805e-03	0	762863	603105	6.33079e-05	3	159	4	82
24qubits_07	56	80	4.06535e-03	0	659716	711486	9.45728e-05	4	37	3	0
24qubits_08	56	215	6.59156e-03	1	885413	291401	1.74522e-05	1	247	4	81
24qubits_09	56	716	7.29064e-03	0	401350	929361	6.82934e-05	5	257	2	65
28qubits_01	98700	1000	6.58567e-03	0	615787	300938	1.04770e-05	8	224	4	98
28qubits_00	98700	197	1.42217e-03	1	460054	209518	7.62522e-05	7	287	3	54
28qubits_02	98700	531	5.88032e-03	1	402352	258683	4.81220e-06	8	277	2	47
28qubits_03	98700	629	4.35568e-03	0	429007	82966	3.89304e-05	8	239	4	8
28qubits_04	98700	698	7.96341e-03	0	221061	633412	7.86532e-05	4	68	4	89

sourced from physics publications) and (2) only classically estimating the Ys for a hyperparameters assignment. Our primary focus is evaluating the algorithm `AccelerQ`, not the ML component.

For ADAPT-QSCI, the MAE and MSE were 6.28776 and 129.512 (for the 10% set) and 6.37912 and 122.659 (for the 20% set), and for QCELS, these were 9.05254, 258.031, 8.25527 and 145.092. These results indicate the need for a custom loss function, some feature weighting, and a validation stage with larger datasets, which we leave for future work.

Table 2: Predicted optimal hyperparameters (A-E cols.) with the first row stating the default values for QCELS implementation (**Size**: the approximate size of the Hamiltonian as a vector of terms, **A**: delta\_t, **B**: n\_Z, **C**: ham\_terms, **D**: ham\_cutoff, and **E**: alpha)

System	Size	A	B	C	D	E
Default	-	0.03	10	200	1e-9	0.8
20qubits_00	63636	1.37929e-01	14	877	6.77275e-03	9.76144e-01
20qubits_01	54717	2.87833e-01	8	69	9.23310e-04	5.26429e-01
20qubits_02	54723	1.05366e-01	10	989	4.31098e-04	8.77018e-01
20qubits_03	54710	1.04235e-01	16	68	6.91101e-03	5.12876e-01
20qubits_04	63636	1.31645e-01	19	971	2.10235e-03	7.76523e-01
20qubits_05	46	1.98379e-01	7	187	8.34526e-03	5.33536e-01
24qubits_05	56	2.08699e-01	24	933	5.75035e-03	6.20185e-01
24qubits_06	56	1.75486e-01	10	398	7.28888e-03	9.72887e-01
24qubits_07	56	1.80166e-01	11	286	1.06348e-03	9.75924e-01
24qubits_08	56	2.72722e-01	22	453	6.67156e-03	8.29813e-01
24qubits_09	56	2.09069e-01	24	650	3.99377e-03	5.20032e-01
28qubits_00	98700	7.00174e-03	7	310	6.71154e-03	6.32763e-01
28qubits_01	98700	1.99713e-01	23	309	8.39957e-03	5.54053e-01
28qubits_02	98700	5.46760e-02	12	997	1.22706e-03	5.60243e-01
28qubits_03	98700	4.23353e-02	6	553	8.40543e-03	8.66162e-01
28qubits_04	98700	2.33005e-01	25	280	1.30071e-04	5.98526e-01

**Optimal Hyperparameters Prediction Results.** Table 1 and Table 2 show the optimal hyperparameters found by `AccelerQ` with each Hamiltonian (System col.) employing the two models above. Size col. is the number of terms in the system. The first row shows the default values of the implementation. Table 1 shows the ADAPT-QSCI’s optimal hyperparameters, with col. A-J represents the predicted optimal hyperparameters values. Similarly, Table 2 presents the optimal hyperparameters for the QCELS implementation in col. A-E. The value presented in Table 1 for the predicted iter\_max

Table 3: Hamiltonian sizes (Size col.) and the size after compression used when querying the ML Models (Comp. col.). The column Comp. represents the size of the system as utilised in the ML model. We marked with an asterisk the open-source molecular Hamiltonians.

System	Size	Comp.	System	Size	Comp.	System	Size	Comp.
20qubits_00	63636	91	24qubits_05(*)	56	48	28qubits_00	98700	167
20qubits_01	54717	287	24qubits_06(*)	56	46	28qubits_01	98700	158
20qubits_02	54723	445	24qubits_07(*)	56	50	28qubits_02	98700	98
20qubits_03	54710	338	24qubits_08(*)	56	51	28qubits_03	98700	144
20qubits_04	63636	65	24qubits_09(*)	56	47	28qubits_04	98700	213
20qubits_05(*)	46	46						

was capped during execution<sup>7</sup> to ensure that we do not have unlimited resources. In practice, the `iter_max` has the same limit as with the default parameters (i.e. `iter_max=1e7/sampling_shots`; col. E and col. D). Table 3 shows the size (Size col.) and the compressed size (Comp. col.) of the Hamiltonians (System col.) used when querying the ML model during prediction, marking with an asterisk the open-source molecular Hamiltonians. Different cutoffs and compression rates were used for ML part than in the QE implementations. Consequentially, the sizes recorded in Table 3 are true only for the ML model.

In Table 3, the number of terms in the open-source molecular Hamiltonians systems ( $\leq 46$ ) is significantly smaller than the challenge Hamiltonians ones ( $\geq 54k$ ), even after compression, the open-source molecular Hamiltonians systems was still much smaller on average. This suggests that these systems may differ to some extent.

The results in Table 1 suggest that the optimisation opted to (sometimes) lower the performance of each iteration, resulting in less precise results per iteration but using more iterations overall by reducing (sometimes) sampling shots and increasing the `atol`, `coeff_cutoff` and `iter_max`. However, when the optimisation predicted both `iter_max` and `sampling_shots` at maximum values, ignoring their correlation, the execution was capped, resulting in fewer iterations in practice.

The results in Table 2 show that the optimisation favoured increasing the number of large coefficients (except for 20qubits\_01 and 20qubits\_03) using larger `ham_cutoff` values and hence leaving fewer small coefficients. Further, the optimisation selected higher values for `n_z` and `delta.t`, with no clear preference for `alpha`.

**Results of Execution with Different Hyperparameters.** Table 4 and Table 5 summarise the results of executing ADAPT-QSCI and QCELS on a quantum simulator with the default and optimal hyperparameters in Table 1 and Table 2. We evaluated predictions on several Hamiltonians of 20-, 24-, and 28-qubit systems (System col.) with a known solution (Value col.). Table 4 presents the result obtained with the challenge Hamiltonians, while Table 5 is the results using the open-source molecular Hamiltonians. Both tables present, for each algorithm and set of hyperparameters (Algorithm col.), the task score (Task Score col.), the approximate run time (Approx. Runtime col.), and the number of iterations completed (Itr. col.). For Table 4, the true results (Value col.) are known [46], and we computed the relative error (Error (%) col.) per experiment. We ran each experiment several times and selected the best result.

In Table 4, the optimised hyperparameters tended to achieve better results than the default. The optimised ADAPT-QSCI found the best solution for 4 systems, optimised QCELS for 3, default QCELS for 2, and default ADAPT-QSCI for 1 out of 10 tested systems. For 20-qubit systems, optimised ADAPT-QSCI had the lowest error at 4.25%, followed by optimised QCELS at 4.27%. Default QCELS and ADAPT-QSCI had average error rates of 4.51% and 4.57%, respectively. For 28-qubit systems, optimised QCELS had the lowest error at 6.42%, followed by optimised ADAPT-QSCI at 6.44%, default ADAPT-QSCI at 6.56%, and default QCELS at 6.58%. Table 5 shows that default parameters performed better. The default ADAPT-QSCI found the best solution for 3 systems, followed by optimised ADAPT-QSCI for 2, and default QCELS for 1 out of 6 tested systems.

**Answer to RQ1.** The results indicate a limited ability to improve solely through hyperparameter optimisation, though the optimised hyperparameters performed better in Table 4. A more refined

<sup>7</sup>The platform automatically stopped the computation once the maximum number of shots, 10 000 000, was reached.

Table 4: Results of execution of ADAPT-QSCI and QCELS with default and optimal hyperparameters (Itr. is Iterations Completed)

System	Value	Algorithm	Error (%)	Task Score	Aprox. Runtime	Itr.
20qubits_00	-22.046059902	ADAPT-QSCI, Opt.	2.46	<b>-21.503637869562557</b>	15777 s	159
		ADAPT-QSCI, Default	4.52	-21.05032811997207	8211 s	97
		QCELS, Opt.	2.57	-21.48036468528949	14991 s	157
		QCELS, Default	4.47	-21.0598063085247	7936 s	92
20qubits_01	-22.046059902	ADAPT-QSCI, Opt.	6.26	-20.66624780754983	4476 s	11
		ADAPT-QSCI, Default	4.49	-21.055920933889066	7463 s	84
		QCELS, Opt.	6.30	-20.655947060040507	4327 s	11
		QCELS, Default	4.30	<b>-21.097506543499456</b>	7486 s	82
20qubits_02	-22.046059902	ADAPT-QSCI, Opt.	5.85	-20.75547153586126	4941 s	12
		ADAPT-QSCI, Default	4.55	<b>-21.042520869027147</b>	6370 s	65
		QCELS, Opt.	5.85	-20.756855659992507	4789 s	12
		QCELS, Default	4.62	-21.02776101198928	6152 s	65
20qubits_03	-22.046059902	ADAPT-QSCI, Opt.	3.37	-21.302881787984727	8631 s	95
		ADAPT-QSCI, Default	4.63	-21.024636461355875	6682 s	77
		QCELS, Opt.	3.27	<b>-21.32597699721156</b>	8575 s	95
		QCELS, Default	4.59	-21.03455240312227	6293 s	66
20qubits_04	-22.046059902	ADAPT-QSCI, Opt.	3.31	<b>-21.316521673460805</b>	11004 s	121
		ADAPT-QSCI, Default	4.64	-21.024150729181112	7595 s	88
		QCELS, Opt.	3.34	-21.308808719093236	9807 s	108
		QCELS, Default	4.57	-21.03798918026242	7039 s	83
28qubits_00	-30.748822808	ADAPT-QSCI, Opt.	6.35	<b>-28.7974854444735</b>	10812 s	48
		ADAPT-QSCI, Default	6.42	-28.77456507714568	10345 s	61
		QCELS, Opt.	6.35	-28.794794630409676	11076 s	48
		QCELS, Default	6.40	-28.779806038153325	10989 s	65
28qubits_01	-30.748822808	ADAPT-QSCI, Opt.	6.39	<b>-28.783766574436143</b>	10024 s	34
		ADAPT-QSCI, Default	6.47	-28.758306955348417	11789 s	77
		QCELS, Opt.	6.41	-28.777776815200454	10096 s	34
		QCELS, Default	6.46	-28.763094962187317	11249 s	74
28qubits_02	-30.748822808	ADAPT-QSCI, Opt.	6.41	-28.778922785865355	11373 s	39
		ADAPT-QSCI, Default	6.68	-28.69374047078425	9479 s	53
		QCELS, Opt.	6.39	<b>-28.7835710030780</b>	10666 s	39
		QCELS, Default	6.66	-28.70067301821086	9509 s	57
28qubits_03	-30.748822808	ADAPT-QSCI, Opt.	6.25	-28.827497968717516	11248 s	51
		ADAPT-QSCI, Default	6.47	-28.75988277903682	12548 s	85
		QCELS, Opt.	6.18	<b>-28.848400001238723</b>	11644 s	53
		QCELS, Default	6.66	-28.699830076240456	11168 s	70
28qubits_04	-30.748822808	ADAPT-QSCI, Opt.	6.79	-28.662288396044573	6757 s	16
		ADAPT-QSCI, Default	6.77	-28.667008949938953	8603 s	43
		QCELS, Opt.	6.78	-28.66351868143365	7463 s	16
		QCELS, Default	6.70	<b>-28.689855023621764</b>	5909 s	45

model based on Hamiltonian characteristics is required to properly assess the optimisation of hyperparameters’ impact on accelerating and improving QE efficiency and accuracy.

In detail: **(20-qubit)** Both implementations, with default or optimised hyperparameters, had similar iteration counts with the default setup consuming less time on average. However, optimised setups performed worse when the number of iterations was too low. **(24-qubit)** Time consumption increased for both ADAPT-QSCI and QCELS with optimised hyperparameters and used fewer iterations when the error percentage was higher than in the default setup. **(28-qubit)** The number of iterations was halved on average, with optimised setups requiring 38 compared to 62-64 iterations with default setups. **For all systems**, optimised hyperparameters used 42-44 iterations versus 53-56 for the default setups, with some increase in time consumption for the optimised setup. 9 systems performed better with optimised setups, while 7 performed better with the default setups, mostly from [Table 5](#).

**Answer to RQ2.** Our understanding of `AccelerQ`’s scalability remains somewhat limited: 80% of the 28-qubit systems’ scores improved with optimised setup, while only 45% of the 20- and 24-qubit systems (5 out of 11) showed improvement. This suggests other factors, like Hamiltonian nature, hyperparameter types, padding, or even data proportions (per source of Hamiltonians), affect scalability and require further investigation.

In detail: [Table 4](#) shows that optimised hyperparameters performed better for the challenge Hamiltonians. We observed the opposite for the open-source molecular Hamiltonians [Table 5](#), particularly for optimised QCELS. The challenge Hamiltonian systems contributed 8.4% of ADAPT-QSCI’s and

Table 5: Results of execution of ADAPT-QSCI and QCELS with default and optimal hyperparameters (Itr. is Iterations Completed)

System	Algorithm	Task Score	Aprox. Runtime	Itr.
20qubits05	ADAPT-QSCI, Opt.	-13.120566186315502	3568 s	27
	ADAPT-QSCI, Default	<b>-14.000000000000009</b>	686 s	9
	QCELS, Opt.	-12.968777862300158	3719 s	26
	QCELS, Default	-14.000000000000004	681 s	9
24qubits05	ADAPT-QSCI, Opt.	-9.034894851637292	3029 s	11
	ADAPT-QSCI, Default	<b>-10.99319108738972</b>	7053 s	35
	QCELS, Opt.	-8.622105677825234	4741 s	8
	QCELS, Default	-9.039194172208862	5367 s	35
24qubits06	ADAPT-QSCI, Opt.	<b>-9.460283005059706</b>	4718 s	8
	ADAPT-QSCI, Default	-9.460283005059702	644 s	6
	QCELS, Opt.	-9.460283005059704	4467 s	8
	QCELS, Default	-9.4602830050597	663 s	6
24qubits07	ADAPT-QSCI, Opt.	-7.34876884915856	4637 s	12
	ADAPT-QSCI, Default	<b>-10.400021274590904</b>	8117 s	37
	QCELS, Opt.	-7.932213481832702	3977 s	10
	QCELS, Default	-9.973622581884937	5117 s	36
24qubits08	ADAPT-QSCI, Opt.	<b>-6.274613702752347</b>	4560 s	35
	ADAPT-QSCI, Default	-6.034877031453911	1516 s	17
	QCELS, Opt.	-5.598926935684615	4779 s	35
	QCELS, Default	-6.034877031453906	1585 s	17
24qubits09	ADAPT-QSCI, Opt.	-13.136457290516125	4660 s	7
	ADAPT-QSCI, Default	-13.136457290516129	649 s	7
	QCELS, Opt.	-13.13645729051612	3941 s	6
	QCELS, Default	<b>-13.13645729051613</b>	686 s	7

37.9% of QCELS’s training data. There is also a correlation between the models: when QCELS with optimised hyperparameters outperformed the default setup, ADAPT-QSCI typically did as well, and vice versa. This suggests that the data each type of Hamiltonian contributed might not be the primary factor. Lastly, the open-source molecular Hamiltonians systems had fewer terms used in the ML phase in comparison to the challenge Hamiltonians, which may affect the model’s ability to generalise<sup>8</sup>.

## 7 Conclusion

In this paper, we presented interdisciplinary work that merges software engineering and machine learning paradigms to enhance quantum algorithms’ performance on NISQ hardware. This idea explored using Hybrid Quantum-Classical Systems as a promising way to utilise current NISQ hardware. While classical computers are essential to optimise noisy quantum hardware, the workload balance should still keep the quantum device at the core of the computation for such systems to stay relevant. The limit between optimising the quantum circuit outcome and bypassing the hardware limitations with classical means is difficult to define; it is however important to keep this balance in mind when developing hybrid systems.

We designed a new framework, implemented as a prototype tool, **AccelerQ**, to predict quantum algorithm (near to) optimal hyperparameters. We evaluated **AccelerQ** on two implementations, training and deploying relatively small-scale models to improve performance by suggesting better hyperparameters. Our results raised the possibility that the model’s ability to predict optimal hyperparameters depends on the Hamiltonian characteristics rather than solely on a specific implementation (ADAPT-QSCI or QCELS).

**Code and Data Availability.** The code, the training data, the models and the results are available as open-source at [7, 8].

**Acknowledgments.** We thank CloudLab [18] for the platform and infrastructure support that enabled the experiment resulting in the construction of two models for accelerating quantum algorithms. Sophie Fortz, Connor Lenihan and Avner Bensoussan are partially supported by the EPSRC project on Verified Simulation for Large Quantum Systems (VSL-Q), grant reference EP/Y005244/1. Sophie

<sup>8</sup>Open-source molecular Hamiltonians averaged 48.2 elements, compared to 200.6 for the challenge Hamiltonians, Table 3.

Fortz and Avner Bensoussan are partially funded by the EPSRC project on Robust and Reliable Quantum Computing (RoarQ), Investigation 009. Sophie is partially funded by Model-based monitoring and calibration of quantum computations (ModeMCQ), grant reference EP/W032635/1 and by the QAssure project from Innovate UK. Also King’s Quantum grants provided by King’s College London are gratefully acknowledged.

## References

- [1] G. Acampora, F. Di Martino, A. Massa, R. Schiattarella, and A. Vitiello. D-nisq: A reference model for distributed noisy intermediate-scale quantum computers. *Information Fusion*, 89:16–28, 2023. ISSN 1566-2535. doi: <https://doi.org/10.1016/j.inffus.2022.08.003>. URL <https://www.sciencedirect.com/science/article/pii/S1566253522000951>.
- [2] M. A. al Badri, E. Linscott, A. Georges, D. J. Cole, and C. Weber. Superexchange mechanism and quantum many body excitations in the archetypal di-cu oxo-bridge. *Communications Physics*, 3(1):4, 2020. doi: 10.1038/s42005-019-0270-1. URL <https://doi.org/10.1038/s42005-019-0270-1>.
- [3] F. Arute, K. Arya, R. Babbush, D. Bacon, J. C. Bardin, R. Barends, R. Biswas, S. Boixo, F. G. S. L. Brandao, D. A. Buell, B. Burkett, Y. Chen, Z. Chen, B. Chiaro, R. Collins, W. Courtney, A. Dunsworth, E. Farhi, B. Foxen, A. Fowler, C. Gidney, M. Giustina, R. Graff, K. Guerin, S. Habegger, M. P. Harrigan, M. J. Hartmann, A. Ho, M. Hoffmann, T. Huang, T. S. Humble, S. V. Isakov, E. Jeffrey, Z. Jiang, D. Kafri, K. Kechedzhi, J. Kelly, P. V. Klimov, S. Knysh, A. Korotkov, F. Kostriksa, D. Landhuis, M. Lindmark, E. Lucero, D. Lyakh, S. Mandrà, J. R. McClean, M. McEwen, A. Megrant, X. Mi, K. Michielsen, M. Mohseni, J. Mutus, O. Naaman, M. Neeley, C. Neill, M. Y. Niu, E. Ostby, A. Petukhov, J. C. Platt, C. Quintana, E. G. Rieffel, P. Roushan, N. C. Rubin, D. Sank, K. J. Satzinger, V. Smelyanskiy, K. J. Sung, M. D. Trevithick, A. Vainsencher, B. Villalonga, T. White, Z. J. Yao, P. Yeh, A. Zalcman, H. Neven, and J. M. Martinis. Quantum supremacy using a programmable superconducting processor. *Nature*, 574(7779):505–510, Oct. 2019. ISSN 1476-4687. doi: 10.1038/s41586-019-1666-5. URL <https://www.nature.com/articles/s41586-019-1666-5>. Number: 7779 Publisher: Nature Publishing Group.
- [4] C. H. Bennett and G. Brassard. Quantum public key distribution reinvented. *SIGACT News*, 18(4):51–53, jul 1987. ISSN 0163-5700. doi: 10.1145/36068.36070. URL <https://doi.org/10.1145/36068.36070>.
- [5] C. H. Bennett, G. Brassard, S. Breidbart, and S. Wiesner. Quantum cryptography, or unforgeable subway tokens. In D. Chaum, R. L. Rivest, and A. T. Sherman, editors, *Advances in Cryptology*, pages 267–275, Boston, MA, 1983. Springer US. ISBN 978-1-4757-0602-4.
- [6] C. H. Bennett, G. Brassard, C. Crépeau, R. Jozsa, A. Peres, and W. K. Wootters. Teleporting an unknown quantum state via dual classical and einstein-podolsky-rosen channels. *Phys. Rev. Lett.*, 70:1895–1899, Mar 1993. doi: 10.1103/PhysRevLett.70.1895. URL <https://link.aps.org/doi/10.1103/PhysRevLett.70.1895>.
- [7] A. Bensoussan, E. Chachkarova, K. Even-Mendoza, S. Fortz, and C. Lenihan. Artifact of Accelerating Quantum Algorithms With Machine Learning (competition code), July 2024. URL <https://doi.org/10.5281/zenodo.12634481>.
- [8] A. Bensoussan, E. Chachkarova, K. Even-Mendoza, S. Fortz, and C. Lenihan. Artifact of Accelerating Quantum Algorithms With Machine Learning, Sept. 2024. URL <https://doi.org/10.5281/zenodo.13328383>.
- [9] H. Berger, A. Dakhama, Z. Ding, K. Even-Mendoza, D. Kelly, H. Menendez, R. Moussa, and F. Sarro. *Stable Yolo: Optimizing Image Generation for Large Language Models*, page 133–139. Springer, Dec. 2023. ISBN 978-3-031-48795-8.

- [10] K. Bharti, A. Cervera-Lierta, T. H. Kyaw, T. Haug, S. Alperin-Lea, A. Anand, M. Degroote, H. Heimonen, J. S. Kottmann, T. Menke, W.-K. Mok, S. Sim, L.-C. Kwek, and A. Aspuru-Guzik. Noisy intermediate-scale quantum (NISQ) algorithms. *Reviews of Modern Physics*, 94(1):015004, Feb. 2022. ISSN 0034-6861, 1539-0756. doi: 10.1103/RevModPhys.94.015004. URL <http://arxiv.org/abs/2101.08448>. arXiv:2101.08448 [cond-mat, physics:quant-ph].
- [11] G. Brassard, P. Høyer, and A. Tapp. *Quantum Algorithm for the Collision Problem*, pages 1662–1664. Springer New York, New York, NY, 2016. ISBN 978-1-4939-2864-4. doi: 10.1007/978-1-4939-2864-4\_304. URL [https://doi.org/10.1007/978-1-4939-2864-4\\_304](https://doi.org/10.1007/978-1-4939-2864-4_304).
- [12] A. E. I. Brownlee, J. Callan, K. Even-Mendoza, A. Geiger, C. Hanna, J. Petke, F. Sarro, and D. Sobania. Enhancing genetic improvement mutations using large language models. In *Search-Based Software Engineering*, pages 153–159, Cham, 2024. Springer Nature Switzerland.
- [13] Connorpl. QAGC\_submission. [https://github.com/Connorpl/QAGC\\_submission](https://github.com/Connorpl/QAGC_submission), Accessed: July 4, 2024.
- [14] Connorpl. QCELS\_for\_QAGC. [https://github.com/Connorpl/QCELS\\_for\\_QAGC](https://github.com/Connorpl/QCELS_for_QAGC), Accessed: July 4, 2024.
- [15] A. Dakhama, K. Even-Mendoza, W. B. Langdon, H. D. Menéndez, and J. Petke. Searchgem5: Towards reliable gem5 with search based software testing and large language models. In *SS-BSE 2023, Proceedings*, volume 14415 of *LNCS*, pages 160–166, San Francisco, CA, USA, 2023. Springer. doi: 10.1007/978-3-031-48796-5\\_14. Best challenge track paper.
- [16] D. Deutsch and R. Jozsa. Rapid solution of problems by quantum computation. *Proceedings of the Royal Society of London. Series A: Mathematical and Physical Sciences*, 439(1907):553–558, 1992.
- [17] Z. Ding and L. Lin. Even shorter quantum circuit for phase estimation on early fault-tolerant quantum computers with applications to ground-state energy estimation. *PRX Quantum*, 4:020331, May 2023. doi: 10.1103/PRXQuantum.4.020331. URL <https://link.aps.org/doi/10.1103/PRXQuantum.4.020331>.
- [18] D. Duplyakin, R. Ricci, A. Maricq, G. Wong, J. Duerig, E. Eide, L. Stoller, M. Hibler, D. Johnson, K. Webb, A. Akella, K. Wang, G. Ricart, L. Landweber, C. Elliott, M. Zink, E. Cecchet, S. Kar, and P. Mishra. The design and operation of cloudblab. In *Proceedings of the 2019 USENIX Conference on Usenix Annual Technical Conference*, USENIX ATC '19, page 1–14, USA, 2019. USENIX Association. ISBN 9781939133038.
- [19] V. H. S. Durelli, R. S. Durelli, S. S. Borges, A. T. Endo, M. M. Eler, D. R. C. Dias, and M. P. Guimarães. Machine learning applied to software testing: A systematic mapping study. *IEEE Transactions on Reliability*, 68(3):1189–1212, 2019. doi: 10.1109/TR.2019.2892517.
- [20] A. Fan, B. Gokkaya, M. Harman, M. Lyubarskiy, S. Sengupta, S. Yoo, and J. M. Zhang. Large language models for software engineering: Survey and open problems. In *2023 IEEE/ACM International Conference on Software Engineering: Future of Software Engineering (ICSE-FoSE)*, pages 31–53, 2023. doi: 10.1109/ICSE-FoSE59343.2023.00008.
- [21] D. Fastovets, Y. Bogdanov, B. Bantysh, and V. Lukichev. Machine learning methods in quantum computing theory. In V. F. Lukichev and K. V. Rudenko, editors, *International Conference on Micro- and Nano-Electronics 2018*, page 85, Zvenigorod, Russian Federation, Mar. 2019. SPIE. ISBN 978-1-5106-2709-3 978-1-5106-2710-9. doi: 10.1117/12.2522427. URL <https://www.spiedigitallibrary.org/conference-proceedings-of-spie/11022/2522427/Machine-learning-methods-in-quantum-computing-theory/10.1117/12.2522427.full>.
- [22] R. P. Feynman. Simulating physics with computers. *International Journal of Theoretical Physics*, 21(6/7), 1982.
- [23] J. H. Friedman. Greedy function approximation: a gradient boosting machine. *Annals of statistics*, pages 1189–1232, 2001.



- [24] I.-D. Gheorghe-Pop, N. Tcholtchev, T. Ritter, and M. Hauswirth. Quantum DevOps: Towards Reliable and Applicable NISQ Quantum Computing. In *2020 IEEE Globecom Workshops (GC Wkshps*, pages 1–6, Taipei, Taiwan, Dec. 2020. IEEE. ISBN 978-1-72817-307-8. doi: 10.1109/GCWkshps50303.2020.9367411. URL <https://ieeexplore.ieee.org/document/9367411/>.
- [25] F. Greiwe, T. Krüger, and W. Maurerer. Effects of Imperfections on Quantum Algorithms: A Software Engineering Perspective, Aug. 2023. URL <http://arxiv.org/abs/2306.02156>. arXiv:2306.02156 [cs].
- [26] H. R. Grimsley, S. E. Economou, E. Barnes, and N. J. Mayhall. An adaptive variational algorithm for exact molecular simulations on a quantum computer. *Nature Communications*, 10(1):3007, July 2019. ISSN 2041-1723. doi: 10.1038/s41467-019-10988-2. URL <http://arxiv.org/abs/1812.11173>. arXiv:1812.11173 [cond-mat, physics:physics, physics:quant-ph].
- [27] L. K. Grover. A fast quantum mechanical algorithm for database search, Nov. 1996. URL <http://arxiv.org/abs/quant-ph/9605043>. arXiv:quant-ph/9605043.
- [28] M. Harman. The role of artificial intelligence in software engineering. In *2012 First International Workshop on Realizing AI Synergies in Software Engineering (RAISE)*, pages 1–6, 2012. doi: 10.1109/RAISE.2012.6227961.
- [29] M. Harman and B. F. Jones. Search-based software engineering. *Information and Software Technology*, 43(14):833–839, 2001. ISSN 0950-5849. doi: [https://doi.org/10.1016/S0950-5849\(01\)00189-6](https://doi.org/10.1016/S0950-5849(01)00189-6). URL <https://www.sciencedirect.com/science/article/pii/S0950584901001896>.
- [30] S. Huang, K. Yang, S. Qi, and R. Wang. When large language model meets optimization. *arXiv preprint arXiv:2405.10098*, 2024.
- [31] K. Kanno, M. Kohda, R. Imai, S. Koh, K. Mitarai, W. Mizukami, and Y. O. Nakagawa. Quantum-selected configuration interaction: Classical diagonalization of hamiltonians in subspaces selected by quantum computers. *arXiv preprint arXiv:2302.11320*, 2023.
- [32] K. Kanno, M. Kohda, R. Imai, S. Koh, K. Mitarai, W. Mizukami, and Y. O. Nakagawa. Quantum-selected configuration interaction: classical diagonalization of hamiltonians in subspaces selected by quantum computers, 2023. URL <https://arxiv.org/abs/2302.11320>.
- [33] B. P. Lanyon, J. D. Whitfield, G. G. Gillett, M. E. Goggin, M. P. Almeida, I. Kassal, J. D. Biamonte, M. Mohseni, B. J. Powell, M. Barbieri, A. Aspuru-Guzik, and A. G. White. Towards quantum chemistry on a quantum computer. *Nature Chemistry*, 2(2):106–111, 2010.
- [34] J. W. Z. Lau, K. H. Lim, H. Shrotriya, and L. C. Kwek. NISQ computing: where are we and where do we go? *AAPPS Bulletin*, 32(1):27, Sept. 2022. ISSN 2309-4710. doi: 10.1007/s43673-022-00058-z. URL <https://doi.org/10.1007/s43673-022-00058-z>.
- [35] H. Lim, D. H. Kang, J. Kim, A. Pellow-Jarman, S. McFarthing, R. Pellow-Jarman, H.-N. Jeon, B. Oh, J.-K. K. Rhee, and K. T. No. Fragment molecular orbital-based variational quantum eigensolver for quantum chemistry in the age of quantum computing. *Scientific Reports*, 14(1):2422, 2024.
- [36] K. Maharana, S. Mondal, and B. Nemade. A review: Data pre-processing and data augmentation techniques. *Global Transitions Proceedings*, 3(1):91–99, 2022.
- [37] S. McArdle, S. Endo, A. Aspuru-Guzik, S. C. Benjamin, and X. Yuan. Quantum computational chemistry. *Rev. Mod. Phys.*, 92:015003, Mar 2020. doi: 10.1103/RevModPhys.92.015003. URL <https://link.aps.org/doi/10.1103/RevModPhys.92.015003>.
- [38] A. Mikołajczyk and M. Grochowski. Data augmentation for improving deep learning in image classification problem. In *2018 international interdisciplinary PhD workshop (IIPhDW)*, pages 117–122. IEEE, 2018.

- [39] A. Miranskyy and L. Zhang. On Testing Quantum Programs. In *2019 IEEE/ACM 41st International Conference on Software Engineering: New Ideas and Emerging Results (ICSE-NIER)*, pages 57–60, May 2019. doi: 10.1109/ICSE-NIER.2019.00023. URL <http://arxiv.org/abs/1812.09261>. arXiv:1812.09261 [quant-ph].
- [40] Y. O. Nakagawa, M. Kamoshita, W. Mizukami, S. Sudo, and Y. ya Ohnishi. Adapt-qsci: Adaptive construction of input state for quantum-selected configuration interaction, 2023. URL <https://arxiv.org/abs/2311.01105>.
- [41] D. Peral-García, J. Cruz-Benito, and F. J. García-Peñalvo. Systematic literature review: Quantum machine learning and its applications. *Computer Science Review*, 51:100619, Feb. 2024. ISSN 1574-0137. doi: 10.1016/j.cosrev.2024.100619. URL <https://www.sciencedirect.com/science/article/pii/S1574013724000030>.
- [42] A. Peruzzo, J. McClean, P. Shadbolt, M.-H. Yung, X.-Q. Zhou, P. J. Love, A. Aspuru-Guzik, and J. L. O’Brien. A variational eigenvalue solver on a quantum processor. *Nature Communications*, 5(1):4213, July 2014. ISSN 2041-1723. doi: 10.1038/ncomms5213. URL <http://arxiv.org/abs/1304.3061>. arXiv:1304.3061 [physics, physics:quant-ph].
- [43] J. Preskill. Quantum Computing in the NISQ era and beyond. *Quantum*, 2:79, Aug. 2018. ISSN 2521-327X. doi: 10.22331/q-2018-08-06-79. URL <http://arxiv.org/abs/1801.00862>. arXiv:1801.00862 [cond-mat, physics:quant-ph].
- [44] QunaSys. Qunasys. <https://qunasys.com/en/>, Accessed: July 4, 2024.
- [45] QunaSys. Quantum algorithm grand challenge 2023 (QAGC2023). <https://github.com/QunaSys/quantum-algorithm-grand-challenge-2023>, February 1, 2023.
- [46] QunaSys. Quantum algorithm grand challenge 2024 (QAGC2024). <https://github.com/QunaSys/quantum-algorithm-grand-challenge-2024>, February 1, 2024.
- [47] QunaSys. Prohibited items, quantum algorithm grand challenge 2024 (QAGC2024). <https://github.com/QunaSys/quantum-algorithm-grand-challenge-2024?tab=readme-ov-file#prohibited-items->, February 1, 2024.
- [48] A. Rosenfeld, O. Kardashov, and O. Zang. Automation of android applications functional testing using machine learning activities classification. In *Proceedings of the 5th International Conference on Mobile Software Engineering and Systems, MOBILESoft ’18*, page 122–132, New York, NY, USA, 2018. Association for Computing Machinery. ISBN 9781450357128. doi: 10.1145/3197231.3197241. URL <https://doi.org/10.1145/3197231.3197241>.
- [49] P. W. Shor. Polynomial-Time Algorithms for Prime Factorization and Discrete Logarithms on a Quantum Computer. *SIAM Journal on Computing*, 26(5):1484–1509, Oct. 1997. ISSN 0097-5397, 1095-7111. doi: 10.1137/S0097539795293172. URL <http://arxiv.org/abs/quant-ph/9508027>. arXiv:quant-ph/9508027.
- [50] C. Shorten and T. M. Khoshgoftaar. A survey on image data augmentation for deep learning. *Journal of big data*, 6(1):1–48, 2019.
- [51] J. Tilly, H. Chen, S. Cao, D. Picozzi, K. Setia, Y. Li, E. Grant, L. Wossnig, I. Rungger, G. H. Booth, and J. Tennyson. The Variational Quantum Eigensolver: a review of methods and best practices. *Physics Reports*, 986:1–128, Nov. 2022. ISSN 03701573. doi: 10.1016/j.physrep.2022.08.003. URL <http://arxiv.org/abs/2111.05176>. arXiv:2111.05176 [quant-ph].
- [52] J. Wang, L. Perez, et al. The effectiveness of data augmentation in image classification using deep learning. *Convolutional Neural Networks Vis. Recognit*, 11(2017):1–8, 2017.
- [53] J. Wang, Y. Huang, C. Chen, Z. Liu, S. Wang, and Q. Wang. Software testing with large language models: Survey, landscape, and vision. *IEEE Transactions on Software Engineering*, 2024.
- [54] Y. Wang and J. Liu. A comprehensive review of Quantum Machine Learning: from NISQ to Fault Tolerance, Mar. 2024. URL <http://arxiv.org/abs/2401.11351>. arXiv:2401.11351 [quant-ph, stat].

- [55] C. A. Welty and P. G. Selfridge. Artificial intelligence and software engineering: Breaking the toy mold. *Automated Software Engineering*, 4(3):255–270, 1997. doi: 10.1023/A:1008662625094. URL <https://doi.org/10.1023/A:1008662625094>.
- [56] S. C. Wong, A. Gatt, V. Stamatescu, and M. D. McDonnell. Understanding data augmentation for classification: when to warp? In *2016 international conference on digital image computing: techniques and applications (DICTA)*, pages 1–6. IEEE, 2016.
- [57] xgboost developers. Xgboost tutorials. <https://xgboost.readthedocs.io/en/stable/tutorials/model.html>, 2022.
- [58] D. Zhang and J. J. P. Tsai. Machine learning and software engineering. *Software Quality Journal*, 11(2):87–119, 2003. doi: 10.1023/A:1023760326768. URL <https://doi.org/10.1023/A:1023760326768>.
- [59] I. Šupić and J. Bowles. Self-testing of quantum systems: a review. *Quantum*, 4:337, Sept. 2020. ISSN 2521-327X. doi: 10.22331/q-2020-09-30-337. URL <http://arxiv.org/abs/1904.10042>. arXiv:1904.10042 [quant-ph].